Proton MR Spectroscopic Imaging Depicts Diffuse Axonal Injury in Children with Traumatic Brain Injury

Barbara A. Holshouser, Karen A. Tong, and Stephen Ashwal

BACKGROUND AND PURPOSE: Diffuse axonal injury (DAI) after traumatic brain injury (TBI) is important in patient assessment and prognosis, yet they are underestimated with conventional imaging techniques. We used MR spectroscopic imaging (MRSI) to detect DAI and determine whether metabolite ratios are accurate in predicting long-term outcomes and to examine regional differences in injury between children with TBI and control subjects.

METHODS: Forty children with TBI underwent transverse proton MRSI through the level of the corpus callosum within 1–16 days after injury. T2-weighted, fluid-attenuated inversion recovery, and susceptibility-weighted MR imaging was used to identify voxels as normal-appearing or as nonhemorrhagic or hemorrhagic injury. Neurologic outcome was evaluated at 6–12 months after injury. Metabolite ratios for total (all voxels), normal-appearing, and hemorrhagic brain were compared and used in a logistic regression model to predict long-term outcome. Total and regional metabolite ratios were compared with control data.

RESULTS: A significant decrease in *N*-acetylaspartate (NAA)/creatine (Cr) and increase in choline (Cho)/Cr (evidence of DAI) was observed in normal-appearing ($P < .05$) and visibly injured (hemorrhagic) brain ($P < .001$) compared with controls. In normal-appearing brain NAA/Cr decreased more in patients with poor outcomes (1.32 ± 0.54) than in those with good outcomes (1.61 ± 0.50, $P = .01$) or control subjects (1.86 ± 0.1, $P = .00$). In visibly injured brains, ratios were similarly altered in all patients. In predicting outcomes, ratios from normal-appearing and visibly-injured brain were 85% and 67% accurate, respectively.

CONCLUSION: MRSI can depict injury in brain that appears normal on imaging and is useful for predicting long-term outcomes.

Diffuse axonal injury (DAI) is universally recognized as a consequence of most forms of traumatic brain injury (TBI). The pathology of DAI is histologically characterized by widespread damage to axons in several brain regions, including the brainstem and parasagittal white matter; hallmark hemorrhagic lesions in the corpus callosum (CC); and the gray matter–white matter junctions of the cerebral cortex (1–4). In their immunohistochemical study, Gorrie et al (5) concluded that the extent and distribution of axonal injury resulting from TBI appears similar in children and in adults.

Because of the widespread consequences of DAI, its detection is important for evaluating and treating

patients with TBI and for determining their prognosis. Fortunately, MR imaging has substantially improved our ability to detect hemorrhagic and nonhemorrhagic lesions (6–8). Newer gradient-echo methods have further improved the detection of susceptibility-related effects of hemorrhagic shearing injury (9–13).

Another method, proton MR spectroscopy (MRS) with use of metabolite information from various brain regions enables sensitive, noninvasive assessment of neurochemical alterations after brain injury and can potentially provide early prognostic information regarding clinical outcomes in children with head injury (14–16). MRS studies have shown its use in detecting DAI (17, 18). Ross et al (17) suggested that elevated choline (Cho) levels in white matter may be due to breakdown products appearing after the shearing of myelin and cellular membranes and that reduced *N*-acetylaspartate (NAA) values result from axonal injury. Investigators specifically looking at the splenium of the CC in patients with brain injury found decreased NAA levels (18, 19).

Two-dimensional (2D) MRS imaging (MRSI) or chemical-shift imaging is a technique that allows the simultaneous acquisition of multiple spectra through a defined plane in the brain. Preliminary studies of this technique in TBI show that NAA-derived ratios averaged from all voxels are significantly decreased in children with poor outcomes and that voxels containing hemorrhage, as seen on 2D gradient-echo images, have NAA/creatine (Cr) ratios lower than ratios in voxels that did not (20). Other investigators have used chemical-shift imaging to study brain injury. Macmillan et al (21) studied normal and abnormal areas of brain, as seen on T2-weighted images, in patients with TBI with or without subarachnoid hemorrhage and found low NAA levels in both areas, as compared with control subjects. They also found increased Cho and Cr levels in patients with subarachnoid hemorrhage but no lactate (Lac) to indicate ischemic neurochemical changes. Another study demonstrated a uniform, global reduction of NAA in patients with head injury that returned to normal in those who made a good recovery (22). One study of volumetric proton spectroscopic imaging in 14 subjects with mild TBI showed significant reductions in NAA/Cr and NAA/Cho ratios and increases in Cho/Cr ratios, compared with control subjects, in regions in which brain appeared normal on conventional MR images; however, pooled metabolite ratios were not correlated with 6-month neurologic outcomes (23).

We performed MRSI in patients with mild-to-severe TBI to simultaneously acquire spectra from normal-appearing brain (i.e., brain with no evidence of injury on MR images) and in brain that appears visibly injured on a transverse section through the level of the CC. This area of the brain is where postmortem examination often shows evidence of microscopic evidence of DAI. Voxels in visibly injured brain were determined on the basis of hemorrhagic lesions detected with a new 3D high-resolution susceptibility-weighted imaging (SWI) sequence (9, 10). This sequence can depict a larger number and volume of hemorrhagic lesions than conventional 2D gradient-echo images in children and adolescents with posttraumatic DAI (9).

The main purpose of this study was threefold: (1) to compare differences in the degree of injury in visibly injured and in normal-appearing brain, as manifested by altered levels of spectral metabolites (i.e., reduced NAA/Cr and increased Cho/Cr); (2) to determine whether metabolite ratios from visibly injured brain are more accurate than those in normal-appearing brain in predicting outcomes 6–12 months after injury; and (3) to determine how these ratios differ from control values. We also examined data from five brain regions to determine if spectral data reveal regional differences in the severity of injury among patients with good outcomes, those with poor outcomes, and the control group and whether specific regions had patterns of injury that improved the prediction of long-term outcomes.

Methods

Patient Selection and Data Collection

We examined 40 children and adolescents (mean age, 11.2 ± 5.4 years; age range, 1.6–18.4) with TBI admitted to the pediatric or adult intensive care units at Loma Linda University Medical Center, California, between March 2001 and September 2002. The population was a nonconsecutive series of patients with a well-documented clinical history of TBI. Patients were injured as a result of motor vehicle accidents ($n = 18$), pedestrian-versus-automobile accidents ($n = 14$), accidents involving all-terrain vehicles ($n = 5$), assault ($n = 2<$), or falling off a bicycle ($n = 1$). We excluded children with a history of CNS malformation, developmental disability, previous brain injury and those younger than 18 months. This young population was excluded because metabolite levels rapidly change during brain maturation and reach adult levels at approximately 18 months of age (16, 24, 25). Cases of nonaccidental trauma and child abuse were also excluded; in these cases, most of the children were younger than the age of inclusion, and their pattern of injury may be different from those observed in accidental TBI, as evidenced in our own work (14, 15) and that of others (17, 26).

A neurosurgeon or neurologist (S.A.) examined all patients before MR imaging. The children were also part of a larger, ongoing study of the role of MRS for outcome prediction in children and adolescents with various acute CNS insults that our institutional review board had approved. Informed consent was obtained from parents or legal guardians.

We recorded these clinical variables: patient age; initial Glasgow Coma Scale (GCS) score; first determined mean arterial blood pressure; heart rate; arterial blood pH; hematocrit; serum glucose and sodium levels; occurrence of cardiac arrest or fixed and dilated pupils; initial intracranial pressure level if monitored; occurrence of seizures; and number of days in a coma, being ventilated, and in the hospital. We determined discharge outcomes and outcomes at 6–12 months after injury by using the Pediatric Cerebral Performance Category (PCPC) scale (27). The PCPC scale is a 6-point outcome scoring system modified from the Glasgow Outcome Scale (GOS). It is used to quantify overall functional morbidity and cognitive impairment of infants and children. The PCPC was validated in pediatric patients after acute CNS injury, and its results are correlated with other measures of psychometric function (28). The score includes the following outcomes: (1) normal, or the patient can perform all age-appropriate activities; (2) mild disability, or the patient is conscious, alert, and able to interact at most age-appropriate activities, and he or she may have mild neurologic deficit; (3) moderate disability, or conscious, sufficient cerebral function for age-appropriate activities of daily life, but the patient has significant cognitive impairment; (4) severe disability, or the patient is conscious but dependent on others for daily support because of impaired brain function; (5) vegetative state; and (6) death. For analysis, the six PCPCS scores were dichotomized as (1) normal or mild disability or (2) moderate or severe disability or a vegetative state. No patients died.

A group of nine control patients (mean age, 9.6 ± 5.9 years; age range, 2.3–17.7 years) examined during the same time period were also enrolled to enable comparisons with results in patients and with normative data. Three control subjects were healthy volunteers who did not require sedation. The other control subjects were patients with no history of TBI who underwent neuroimaging for an evaluation of clinical neurologic or craniofacial disorders (e.g., headaches, facial hemangiomas, isolated seizure); on examination, their findings were neurologically normal.

MR Imaging

When medically stable, children were transported to the MR imaging suite and were monitored during these studies by

intensive care unit and radiology personnel. All studies were performed by using a circularly polarized head coil with a conventional 1.5-T whole-body imaging system (Magnetom Vision; Siemens Medical Systems, Iselin, NJ).

Routine MR imaging included the following acquisitions: axial dual spin-echo (TR/TE1/TE2/NEX = 2500/22/80/1, 5-mm-thick sections), sagittal T1-weighted spin-echo (TR/TE/NEX = 550/22/4, 5-mm-thick sections), and axial fluid-attenuated inversion recovery (FLAIR, TR/TE/NEX = 9000/110/1, 5-mm-thick sections). SWI was performed and consisted of a strongly susceptibility-weighted, low-bandwidth (78 Hz per pixel) 3D fast low-angle shot sequence (TR/TE = 57/40, flip angle = 20°). First-order flow was compensated in all three orthogonal directions. Sixty-four 2-mm partitions were acquired by using a rectangular FOV (5/8 of 256 mm) and a matrix size of 160 × 512, resulting in a voxel of $1 \times 0.5 \times 2$ mm^3. The SWI sequence included most the cerebral hemispheres and the posterior fossa, with an acquisition time of approximately 9.5 minutes. SWIs were created by using the magnitude and phase images, as previously explained (29). The underlying contrast mechanism is associated with the difference in magnetic susceptibility between oxygenated and deoxygenated hemoglobin that leads to a phase difference between regions containing deoxygenated blood and surrounding tissues and concomitantly to a cancellation of signal intensity. In our setting, SWI was primarily focused on the phase dispersion caused by extravascular deoxyhemoglobin and methemoglobin rather than intravenous deoxyhemoglobin.

A neuroradiologist (K.A.T.) and a pediatric neurologist (S.A.) reviewed the MR images on a workstation routinely used to view images (DS3000; Impax, Agfa Inc., Teterboro, NJ). Hemorrhagic lesions were defined as hypointense foci that were not compatible with vascular, bony, or artifactual structures on SWI. If the etiology of any focus was in doubt, the lesions were not included as hemorrhagic lesions. The total number and volume of hemorrhagic shearing lesions were recorded from the SWIs for the entire brain. In addition, each voxel of the MRSI was examined to determine whether hemorrhagic lesions were visible.

MR Spectroscopy

2D MRSI was performed with a water-suppressed point-resolved spectroscopic sequence with a TR/TE of 3000/144. The multivoxel acquisition was acquired by using a 10-mm-thick section through the level of the CC and by covering portions of the frontal white matter (FWM) and frontal gray matter (FGM) and parieto-occipital white matter (POWM) and parieto-occipital gray matter (POGM) (2–3 mL per voxel). MRSI spectra were subject to postprocessing, which included zero filling to 32k, 1-Hz exponential multiplication, Fourier transformation, zero-order phase correction, and baseline correction (Luise, Numaris VB33D; Siemens) to obtain peak areas for NAA, Cr, Cho, and Lac, if present (identified as an inverted doublet at 1.33 ppm). Peak areas were transferred by means of DICOM to an automatic processing program developed in our laboratory to calculate metabolite ratios (NAA/Cr, NAA/Cho, Cho/Cr, and Lac/Cr). Values were also transferred to a statistical spreadsheet for further analysis. Each spectrum was visually inspected (by B.A.H.) for adequate spectral quality, and metabolite ratios from accepted voxels (up to 64) within a slab were averaged to obtain a pooled mean metabolite ratio (total) for each patient and control subject. Metabolite ratios from voxels containing blood products, as identified on SWI, were averaged and compared with ratios from normal-appearing brain to determine the affect of metabolite ratios from visibly injured brain on assessing long-term outcomes. Voxels containing nonhemorrhagic DAI, as identified on FLAIR images, were not included in the average for normal-appearing brain.

TABLE 1: Clinical variables in dichotomized outcome groups

Variable	Good-Outcome Group* ($n = 30$)	Poor-Outcome Group† ($n = 10$)	P Value
Age (y)	11.7 ± 5.9	9.7 ± 3.3	.20
GCS score	7 ± 4	4 ± 1	.03‡
Duration (d)			
In coma	5 ± 6	11 ± 9	.02‡
Ventilated	6 ± 6	12 ± 6	.01‡
Hospitalized	27 ± 25	50 ± 30	.03‡
Unconsciousness before MRS	4 ± 4	7 ± 3	.01‡
To MRS	7 ± 4	8 ± 4	.20
Hemorrhagic Lesions			
Total number	116 ± 146	302 ± 199	.002‡
Total volume (mm^3)	11271 ± 15730	36007 ± 31936	.002‡

* Normal or mild disability.

† Moderate or severe disability or vegetative state, as based on the Pediatric Cerebral Performance Category Scaled score.

‡ $P \leq .05$, 2-tailed Mann-Whitney test.

For comparison, mean total ratios were obtained for five regions: FWM, FGM, CC, POWM, and POGM.

Statistical Analysis

Nonparametric Mann-Whitney tests or χ^2 analyses were used to determine significant differences between dichotomous outcome groups for all clinical variables. An analysis of variance (ANOVA), with Bonferroni post hoc tests, was used to determine significant differences among hemorrhagic, normal-appearing, and control groups for all metabolite variables. Multiple variable logistic regression was used to determine the value of clinical parameters and metabolite ratios from total, normal-appearing, or visibly injured brain (independent continuous variables) in predicting neurologic dichotomous outcomes. We report these findings from the logistic analyses: accuracy, false-positive results, false-negative results, and Hosmer-Lemeshow goodness-of-fit χ^2 values, and associated significance levels. A P value of $\leq .05$ was considered significant.

Results

Clinical Data

The patients' PCPC scores at 6–12 months after injury were as follows: normal ($n = 14$); mild ($n = 16$), moderate ($n = 7$), or severe ($n = 2$) disability; or vegetative state ($n = 1$). The mean age of the control subjects was not significantly different from that of the patients ($P = .43$, independent t test). After we dichotomized the PCPC scores, 30 patients were considered to have a good outcome, and 10 were considered to have a poor outcome. Table 1 summarizes the clinical variables in the dichotomized outcome groups. Severity of injury, determined by using the GCS score, ranged from 3 to 15 and was significantly different between outcome groups ($P = .03$). Clinical variables related to the length of recovery after injury differed between outcome groups and included the

number of days the patients remained in a coma (P = .02), the number of days they received ventilator support (P = .01), the number of days the patients remained in the hospital (P = .03), and the number of days the patients were unconscious before MRS (P = .01). The interval between injury and MRS was 1–16 days and not significantly different between outcome groups (P = .20). However, the number and volume of hemorrhagic lesions on 3D SWI varied widely for each group and differences were significant (P < .002).

MRSI Findings

MRSI datasets were collected from all patients, and spectra from each voxel for each patient was inspected, localized by region, compared with SWI at the same transverse level to determine whether the voxel contained hemorrhagic lesions, and compared with FLAIR images to determine if the voxel contained nonhemorrhagic DAI lesions. An average of 33 spectra per patient were included in the analyses. Spectra were excluded if they contained chemical-shift artifact or inadequate spectral quality because of poor shimming. In two patients, spectra from regions containing excessive hemorrhage could not be evaluated because of spectral distortion and loss of signal intensity. These regions, though abnormal, are not included in this analysis. In patients with good outcomes, an average of 8.2% of the voxels contained hemorrhagic lesions, and 1.6% contained nonhemorrhagic DAI lesions. In patients with poor outcomes, 27.6% contained hemorrhage, and 2.2% contained nonhemorrhagic lesions. Because the number of nonhemorrhagic DAI lesions observed in the region covered with MRSI were so few (< three per patient) and because they were observed in only 16 of the patients, ratios from these voxels could not be used for statistical comparisons; however, they were included in the total calculations described next.

Total and Regional Mean Metabolite Ratios

Metabolite ratios from every acceptable spectrum collected for the entire transverse section (which included both visibly injured and normal-appearing brain) were averaged to obtain mean total ratios for each patient. As shown in Figure 1, mean total NAA/Cr ratios decreased with the severity of outcome, and Cho/Cr ratios increased for all patients compared with control subjects. Figure 2 shows all three mean total ratios by dichotomized outcomes, demonstrating that NAA-derived ratios were significantly decreased in both outcome groups compared with control subjects (P < .01). Furthermore, NAA/Cr was decreased significantly more in patients with poor outcomes than patients with good outcomes (P < .01). The Cho/Cr ratios from both outcome groups were significantly increased compared with control subjects (P < .01) but not each other (P = 1.0). A similar distribution of metabolite ratios was seen for regional data (Figure 3). In general, differences in CC and white matter regions were more pronounced than those in gray matter. In pa-
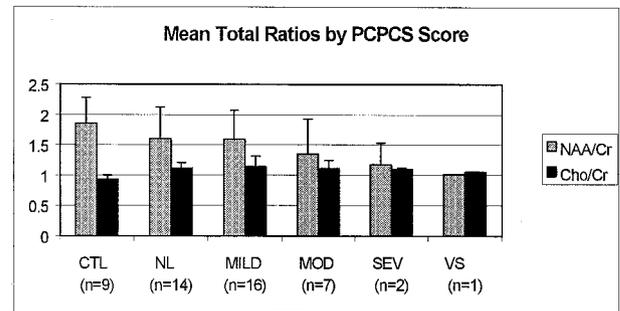
FIG 1. Mean NAA/Cr and Cho/Cr ratios from all voxels plotted as a function of the neurologic outcome assigned by a pediatric neurologist based on the PCPC score 6–12 months after injury. *CTL* indicates control; *MOD*, moderate disability; *NL*, normal; *SEV*, severe disability; and *VS*, vegetative state.
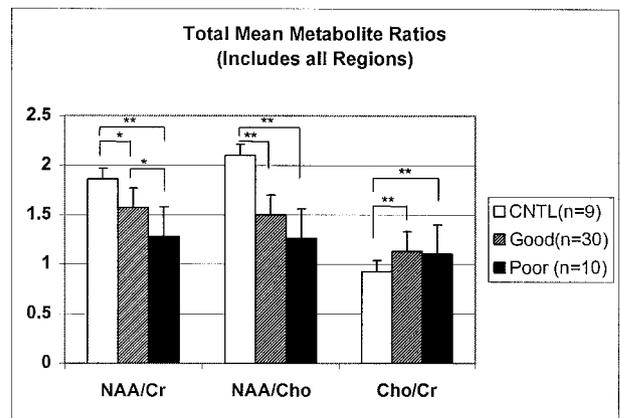
FIG 2. Total mean metabolite ratios plotted by neurologic outcomes or control (*CNTL*). Ratios were calculated from all voxels including those containing hemorrhagic and nonhemorrhagic DAI lesions for patients with TBI. *Asterisk* indicates P = .01; *double asterisk*, P = .000.

tients, NAA/Cr and NAA/Cho metabolite ratios in the CC, FWM, and POWM were significantly decreased compared with those in control subjects (data not shown). NAA/Cr ratios in the CC (P = .02) and POWM (P = .001) were the only ratios that distinguished patient outcome groups. Cho/Cr increased in all regions in patients and was significantly increased in the CC (P < .02) and FWM (P < .02) compared with values in control subjects. We found no significant differences in regional NAA/Cho or Cho/Cr ratios between good- and poor-outcome groups.

Visibly Injured versus Normal-Appearing Brain

Figure 4 shows images and spectral data from a patient with a good outcome (normal) at 12 months after injury. The data illustrate a loss of signal intensity in voxels containing small hemorrhagic lesions and decreased NAA in normal-appearing brain. Images and spectra shown in Figure 5 are from a patient with a poor outcome (severe disabilities) at 12 months after injury. These images illustrate distortion and loss of signal intensity from a large hemorrhagic lesion affecting multiple spectra, as well as a diffuse loss

Regional Mean Metabolite Ratios by Outcome

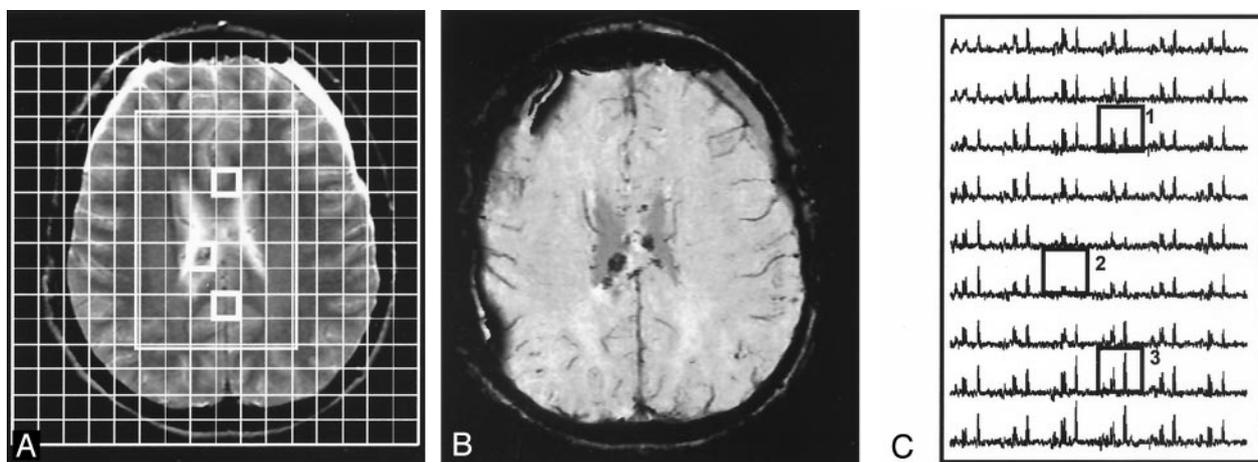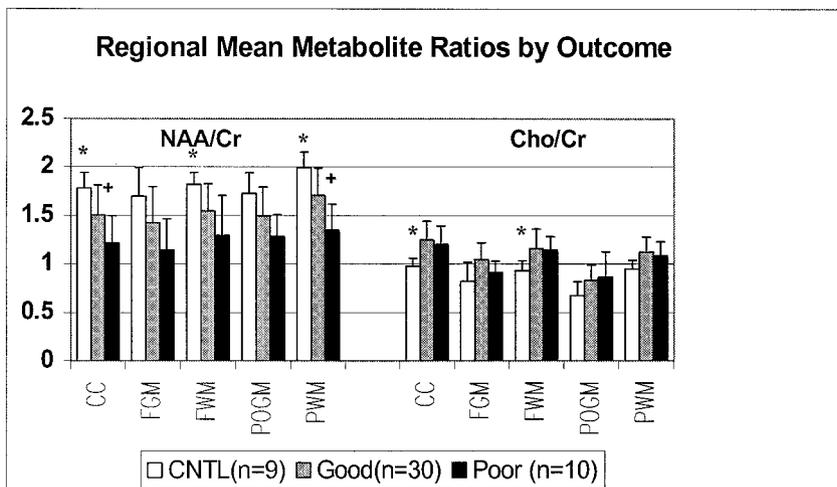□ CNTL(n=9) ▨ Good(n=30) ■ Poor (n=10)

FIG 4. 15-year-old female adolescent ejected from a car. Patient had a good outcome (GOS score = 1, normal) at 12 months after injury. Total mean metabolite ratios are 1.63 (normal) for NAA/Cr, and 1.67 for NAA/Cho, and 1.06 (increased) for Cho/Cr.

A and *B*, T2-weighted MR image (*A*) corresponding SWI (*B*) show hemorrhagic lesions in the body of the CC and bifrontal extra-axial collections. *A* with grid overlay shows the 160-mm FOV and 54 (6 × 9)-voxel volume of interest (*rectangle*). *Boxes* indicate corresponding voxels in *C*.

C, Spectral map from 54 voxels in the volume of interest shows a (1) spectrum from normal-appearing brain in the anterior CC with decreased NAA (2.0 ppm), (2) a spectrum with reduced metabolite signal intensity due to a small hemorrhagic lesion in the mid CC, and (3) a spectrum from parietal white matter with normal metabolite ratios.

of NAA and increased Cho levels in the remaining spectra, with some areas of normal-appearing brain (left frontal and parietal) affected more than others.

Table 2 shows metabolite ratios from all patients, from visibly injured brain (i.e., ratios from voxels in which hemorrhagic lesions were seen on SWI), normal-appearing brain (nonhemorrhagic DAI lesions excluded), and control data. Metabolite ratios from all patients combined were significantly different from those in control subjects ($P \leq .001$). NAA/Cr from visibly injured and normal-appearing brain was significantly decreased compared with the control ratio ($P < .01$), but it was not significantly lower in voxels containing hemorrhage than in those containing normal-appearing brain ($P = .46$). NAA/Cho was significantly decreased between all groups ($P < .001$). As expected, Cho/Cr increased in hemorrhagic brain compared with controls and normal-appearing brain ($P = .00$), and it was also significantly increased in normal-appearing brain compared with control brain ($P = .05$) (Table 2). Lac was detected in visibly-injured areas near large hemorrhagic lesions in four patients.

A comparison of outcome groups by using metabolite ratios in voxels containing hemorrhagic lesions (Fig 6) showed significant differences for all three ratios compared with those in control subjects ($P < .02$). However, we found no significant differences between the good- and poor-outcome groups. A comparison of ratios of spectra from normal-appearing brain (Fig 6) showed that NAA/Cr decreased most in patients with poor outcomes compared with those with good outcomes ($P < .01$), and NAA/Cr in both of these groups was significantly lower than that of control subjects ($P < .02$). NAA/Cho decreased and Cho/Cr increased in normal-appearing brain regardless of the patient's outcome. Therefore, the NAA/Cr ratio from normal-appearing brain was the only ratio
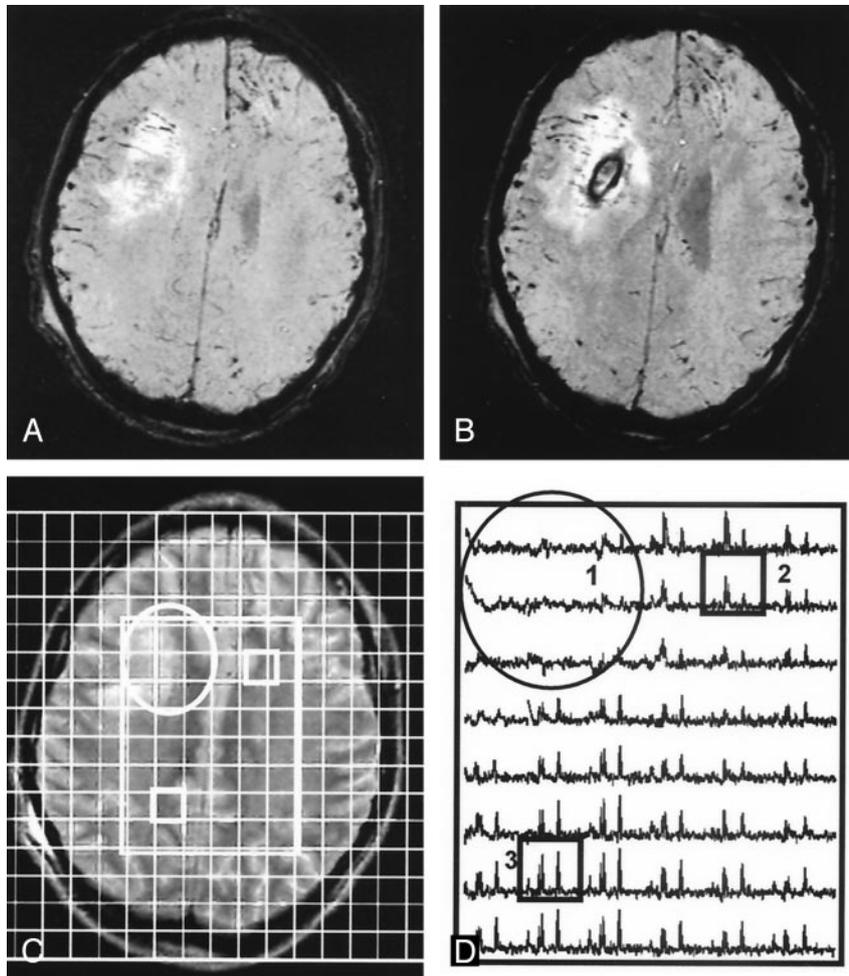
Fig 5. 12-year-old boy hit by a car. Patient had a poor outcome (GOS score = 4, severe disabilities) at 12-month follow-up. Total mean metabolite ratios from MRSI were 1.14 (decreased) for NAA/Cr, 1.13 for NAA/Cho, and 1.11 (increased) Cho/Cr.

A and *B*, Contiguous SWI images show a moderately large hemorrhagic lesion in the deep right frontal lobe.

C, Corresponding T2-weighted MR image shows the lesion (*circle*) with an overlay of the volume of interest (*rectangle*). *Boxes* indicate corresponding voxels in *D*.

D, Spectral map shows loss of metabolite signal intensity in area of the lesion (*circle*) and (2) a spectrum from normal-appearing left FWM with markedly decreased NAA/Cr and increased Cho/Cr, as compared with (3) a spectrum from normal-appearing parietal white matter with decreased NAA/Cr and normal Cho/Cr.

TABLE 2: Mean metabolite ratios

MRSI Ratio	Control ($n = 9$)	TBI ($n = 40$)	Normal-Appearing Brain ($n = 40$)	Visible Hemorrhage ($n = 33$)	P Value*
NAA/Cr	1.86 ± 0.11	$1.50 \pm 0.29^{\dagger}$	$1.55 \pm 0.52^{\ddagger}$	$1.33 \pm 0.56^{\dagger}$	.46
NAA/Cho	2.10 ± 0.19	$1.44 \pm 0.34^{\dagger}$	$1.52 \pm 0.58^{\dagger}$	$1.16 \pm 0.50^{\dagger}$	$.001^{\dagger}$
Cho/Cr	0.93 ± 0.07	$1.12 \pm 0.13^{\dagger}$	$1.10 \pm 0.39^{\ddagger}$	$1.24 \pm 0.51^{\dagger}$	$.00^{\dagger}$

Note.—Ratios are average of mean ratios from each patient. Seven patients did not have voxels containing hemorrhage in the brain section sampled with MRSI.

* Normal versus hemorrhage.

[†] $P \leq .001$ compared with controls, one-way ANOVA and post-hoc Bonferroni test.

[‡] $P \leq 0.05$ level compared to controls, one-way ANOVA and post-hoc Bonferroni test.

that helped to differentiate between good- and poor-outcome groups.

Outcome Prediction

Table 3 shows the results of logistic regression analyses to predict outcomes. Although several MRS ratios alone or in combination correctly predicted a high percentage of outcomes, only a few approached significance on χ^2 testing. Metabolite ratios from normal-appearing brain resulted in 85% predictive accuracy, with one false-positive case, as compared with ratios from brain containing hemorrhage, which had 67% accuracy, with three false-positive cases. Use of mean total ratios, which included ratios from all voxels, resulted in the same predictive accuracies as those of ratios from normal-appearing brain, with less significance. Predictive accuracy with regional metabolite ratios showed that, in general, ratios from white matter regions (POWM = 85%, FWM = 83%, anterior CC = 82%) were more predictive of outcome than ratios from gray matter (FGM = 83%, POGM = 78%). However, none of the predictions reached significance.

Predictive accuracies ranged from 75% for GCS alone to 80% for a combination of clinical variables (days of unconsciousness before MR imaging, days in coma and days receiving ventilator support). The

Fɪɢ 6.   Mean metabolite ratios from visibly injured (hemorrhagic, *Hem*) brain and normal-appearing (*Nrm*) brain were significantly different from those in control subjects (*CNTL*). *Asterisk* indicates $P < .02$. NAA/Cr from normal-appearing brain was the only ratio that differentiates between good- and poor- outcome groups; + indicates $P = .01$.
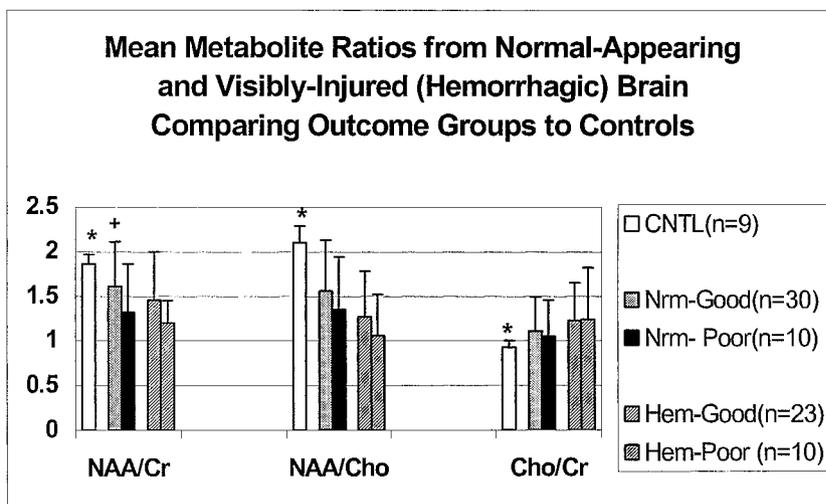

TABLE 3: Results of logistic regression analyses to predict dichotomized GOS outcomes at 6–12 mo

Variables	Accuracy (%)	Predictions False-Positive (%)	False-Negative Rate (%)	χ^2	P Value
GCS score	75	0	100	5.2	.40
Days unconscious before MRS and days ventilated	78	3	80	4.5	.81
Days in coma, unconscious before MRS, and ventilated	80	7	60	8.4	.39
MRS ratios*					
Normal-appearing brain	85	3	50	10.7	.22
Hemorrhagic brain	67	13	80	7.3	.50
Total brain	85	3	50	5.4	.72
Total NAA/Cr, days unconscious before MRS and ventilated	88	3	40	11.2	.19

* Total mean NAA/Cr, NAA/Cho, and Cho/Cr.

highest predictive accuracy was achieved by combining the total mean NAA/Cr ratio with the days of unconsciousness before MR imaging (88%, three false-positive cases), although the result was not significant.

Discussion

Brain trauma produces a diverse spectrum of injuries in which DAI is a well-recognized major contributing factor to long-term disability. MR imaging and CT have long been thought to cause underestimation of the extent of DAI because of their lack of sensitivity; therefore, newer and more sensitive imaging techniques have been developed. Using these techniques with MRSI, we found that MRS is sensitive for DAI in injured areas and normal-appearing areas, as it demonstrated reduced NAA and increased Cho levels in this series of 40 children with-mild to severe TBI.

The metabolite peak commonly described as Cho or total Cho is actually composed of several Cho compounds, including phosphorylcholine and glycerophosphorylcholine. Acceleration/deceleration and rotational forces incurred during TBI are pathologically important factors in axonal shearing injury (30). Cho is thought to be one of the breakdown products of membrane disruption; therefore, increased Cho

levels seen after TBI have been attributed to DAI. In this study, Cho significantly increased in all patients compared with control subjects but not in patients with poor outcomes versus those with good outcomes. This observation may have occurred because the area of the brain assessed (through the level of the CC) is particularly vulnerable to DAI and often where lesions are detected on imaging. Cho/Cr ratios were increased in areas of visibly injured brain, and we also found that Cho levels increased in areas that appeared normal on imaging, illustrating the increased sensitivity of MRS over MR imaging in detecting axonal injury. This finding agrees with another report that also showed increased Cho/Cr in normal-appearing white matter that was not correlated with outcome and stayed elevated in a subgroup of patients examined after 6.2 months (31). Other studies in adults with TBI have shown that Cho values recover to control levels 6–12 months after injury, even in patients with poor outcomes, whereas NAA did not (18, 32, 33). The early elevation in Cho values appears to show the extent of injury, and it may give clinicians additional information with which to explain the patient's status soon after injury; however, because these values are elevated in all patients with TBI, they do not help in predicting long-term outcomes. Changes in Cho detected in specific regions may help

in explaining neurologic deficits in patients with mild injury in whom images are normal.

Axonal injury can also produce a decrease in levels of NAA, a neuronal and axonal marker. Decreased NAA values represent either neuronal loss or neuronal dysfunction, because they recover after the resolution of energy failure (34, 35). A temporary drop in NAA after brain injury may be caused by accelerated lipid synthesis involved in myelin repair, or it may result because NAA provides a temporary source of local cellular energy at the site of axonal injury; this temporary drop could precede any loss of NAA as a result of axonal death (18). In the current study, ratios from MRSI voxels containing normal-appearing brain showed significant decreases in NAA/Cr in all patients compared with control subjects; this agreed with previous reports (21, 36). In addition, NAA/Cr ratios were significantly lower in patients with poor outcomes than in those with good outcomes (i.e., evidence of more severe injury). When ratios from voxels containing hemorrhage were compared, none of the ratios was significantly different between these groups. This finding suggests that MRS measurements from visibly injured brain represent focal rather than global assessment of injury and that they tend to cause overestimation of the severity of injury. A study of a small group of patients in whom MRS was performed in areas of contusion illustrates this point. The investigators found metabolite changes and Lac; however, the findings were not correlated with long-term outcomes (37). We also found Lac in a few spectra, though only in voxels from contused areas near large hemorrhagic lesions; this finding occurred in four patients, two of whom had a good outcome.

Our results may have been influenced by technical factors involved in the acquisition and processing of MRSI data. First, for voxels labeled as normal-appearing brain, we attempted to include only those that appeared to contain brain that was not visibly injured on images and that did not contain mostly CSF. No attempt was made to correct for inclusion of small amounts of CSF because we believed it would have little to no effect on the results, as metabolite ratios were used rather than quantitative measurements. Second, voxels were labeled as hemorrhagic if it included any amount of susceptibility artifact thought to be related to blood products. Therefore, the average metabolite ratios for hemorrhagic voxels represented spectroscopic changes due to the varying amounts of hemorrhage they contained. Also, we could not account for voxels with spectra that were too distorted or that contained no measurable metabolites because of large amounts of blood products. This limitation may have caused us to underestimate the overall effect of hemorrhagic damage when we tried to predict outcomes in a few patients. Third, because ratios were used instead of quantitative metabolite levels, changes in Cr may have affected the ratios and may explain why the Cho/Cr ratio was slightly lower in patients with poor outcomes in some regions (Fig 3). Cr is considered a marker of cell

energy metabolism and mitochondrial function. An increased Cr level may be part of a repair mechanism associated with increased mitochondrial function in areas of injury (38). An MRSI study of brain trauma showed increased Cr and Cho values only in patients with TBI and subarachnoid hemorrhage; this finding was attributed to cell-wall turnover (21). Other single-voxel quantitative studies showed either no significant change in Cr levels (17, 33, 35, 39) or decreased Cr levels (17) compared with control subjects.

In our study, ratios from brain with hemorrhagic lesions at the level of the CC was less accurate than ratios from normal-appearing brain alone in predicting long-term neurologic outcomes, and they falsely predicted more poor outcomes (13% vs 3%). Adding the number of days the patients were unconscious before MRS to the total mean NAA/Cr ratio slightly improved prediction accuracy from 85% to 88%; however, none of the analyses achieved significance, and the results should be interpreted carefully. Given the diffuse nature of TBI, 3D MRSI, which covers the entire brain, may be more useful than our 2D MRSI in assessing total brain injury and predicting outcomes. Although a previous 3D MRSI study did not show a correlation with outcome (23), a study of relatively few patients with mild injury showed that 3D MRSI with improved software strategies (40, 41) is feasible in the clinical setting and shows promise for future studies.

On the basis of neuropathologic findings, some authors now consider DAI a misnomer because injury is frequently not diffuse but multifocal, and as such, the term *traumatic axonal injury* has been suggested to be more appropriate (4). MRSI results seem to confirm this suggestion, as metabolite ratios from different areas can range from normal to very abnormal in the same patient, depending on the area sampled. MRSI also appears to depict axonal injury better than imaging alone because metabolite changes suggestive of DAI were seen in areas of normal-appearing brain, even in patients who recovered to their normal status (Fig 1).

Because none of our patients died, we could not confirm DAI histologically. Once this is done, linking MRS and SWI findings to the three grades of DAI in the Adams neuropathologic classification (2) would provide a working model of TBI. MRS metabolite abnormalities would characterize the microscopic changes in white matter seen in grade 1 (mild) DAI, whereas grossly evident focal lesions on SWI would characterize grade 2 (moderate) DAI if they are isolated to the CC, and additional lesions in the dorsolateral rostral brainstem would define grade 3 (severe) DAI. Such a neuroimaging grading system, linked to the underlying neuropathology, might be sufficiently sensitive and specific to be clinically useful for determining long-term prognoses.

The potential value of combining these different neuroimaging techniques might be of particular importance as more data are collected, particularly in reference to the regional evaluation of metabolite changes. For example, if regional metabolite abnormalities (e.g., frontal or temporal lobes, CC) are cor-

related with specific behavioral, neuropsychological, or neurologic deficits, this information could potentially lead to earlier recognition of such problems and much earlier intervention and treatment.

Conclusion

Proton MRSI depicted metabolite changes suggestive of DAI in areas of brain that appeared normal on imaging. The changes were more accurate for predicting long-term outcomes than ratios from visibly injured brain.

References

1. Adams JH, Graham DI, Murray LS, Scott G. **Diffuse axonal injury due to nonmissile head injury in humans: an analysis of 45 cases.** *Ann Neurol* 1982;12:557–563
2. Adams JH, Doyle D, Ford I, Gennarelli TA, Graham DI, McLellan DR. **Diffuse axonal injury in head injury: definition, diagnosis and grading.** *Histopathology* 1989;15:49–59
3. Graham DI, McIntosh TK, Maxwell WL, et al. **Recent advances in neurotrauma.** *J Neuropathol Ex Neuro* 2000;59:641–651
4. Meythaler JM, Peduzzi JD, Eleftheriou E, Novack TA. **Current concepts: diffuse axonal injury-associated traumatic brain injury.** *Arch Phys Med Rehabil* 2000;82:1461–1471
5. Gorrie C, Oakes S, Duflou J, Blumbergs P, Waite PME. **Axonal injury in children after motor vehicle crashes: Extent, distribution, and size of axonal swellings using β-APP immunohistochemistry.** *J Neurotrauma* 2002;19:1171–1182
6. Gentry LR, Godersky JC, Thompson B. **MR imaging of head trauma: review of the distribution and radiopathologic features of traumatic lesions.** *AJR Am J Roentgenol* 1988;150:663–672
7. Orrison WW, Gentry LR, Stimac GK, Tarrell RM, Espinosa MC, Cobb LC. **Blinded comparison of cranial CT and MR in closed head injury evaluation.** *Am J Neuroradiol* 1994;15:351–356
8. Levin HS, Amparo E, Eisenberg HM, et al. **Magnetic resonance imaging and computerized tomography in relation to the neurobehavioral sequelae of mild and moderate head injuries.** *J Neurosurg* 1987;66:706–713
9. Tong KA, Ashwal SA, Holshouser BA, et al. **Hemorrhagic shearing lesions in children and adolescents with posttraumatic diffuse axonal injury: improved detection and initial results.** *Radiology* 2003;227:332–339
10. Tong KA, Ashwal SA, Holshouser BA, et al. **Diffuse axonal injury in children: clinical correlation with MRI hemorrhagic lesions.** *Ann Neurol* 2004;56:36–50
11. Grados MA, Slomine BS, Gerring JP, Vasa R, Bryan N, Denckla MB. **Depth of lesion model in children and adolescents with moderate to severe traumatic brain injury: use of SPGR MRI to predict severity and outcome.** *J Neurol Neurosurg Psychiatry* 2001;70:350–358
12. Yanagawa Y, Tsushima Y, Tokumaru A, et al. **A quantitative analysis of head injury using T2*-weighted gradient-echo imaging.** *J Trauma* 2000;49:272–277
13. Scheid R, Preul C, Gruber O, Wiggins C, Yves von Cramon D. **Diffuse axonal injury associated with chronic traumatic brain injury: Evidence from T2*-weighted gradient-echo imaging at 3T.** *AJNR Am J Neuroradiol* 2003;24:1049–1056
14. Ashwal S, Holshouser BA, Shu S, et al. **Predictive value of proton magnetic resonance spectroscopy in pediatric closed head injury.** *Pediatric Neurol* 2000;23:114–125
15. Brenner T, Freier MC, Holshouser BA, Burley T, Ashwal S. **Predicting neuropsychologic outcome after traumatic brain injury in children.** *Pediatr Neurol* 2003;28:104–114
16. Holshouser BA, Ashwal S, Luh GY, et al. **¹H-MR spectroscopy after acute CNS injury: outcome prediction in neonates, infants and children.** *Radiology* 1997;202:487–496
17. Ross BD, Ernst T, Kreis R, et al. **1H MRS in acute traumatic brain injury.** *J Magn Reson Imaging* 1998;8:829–840
18. Cecil KM, Hills EC, Sandel ME, et al. **Proton magnetic resonance spectroscopy for detection of axonal injury in the splenium of the corpus callosum of brain-injured patients.** *J Neurosurg* 1998;88:795–801
19. Sinson G, Bagley LJ, Cecil KM, et al. **Magnetization transfer imaging and proton MR spectroscopy in the evaluation of axonal injury: Correlation with clinical outcome after traumatic brain injury.** *AJNR Am J Neuroradiol* 2001;22:143–151
20. Choe JS, Ashwal SA, Tong KA, Holshouser BA. **Proton magnetic resonance spectroscopy in children with post-traumatic diffuse axonal injury.** Presented at: 87th Scientific Assembly and Annual Meeting of the Radiological Society of North America, Chicago, IL, November 25–30, 2001
21. Macmillan CS, Wild JM, Wardlaw JM, Andrews PJ, Marchall I, Easton VJ. **Traumatic brain injury and subarachnoid hemorrhage: in vivo occult pathology demonstrated by magnetic resonance spectroscopy may not be "ischaemic": a primary study and review of the literature.** Acta Neurochir (*Wein*) 2002;144:853–862
22. Signoretti S, Marmarou A, Fatouros P, et al. **Application of chemical shift imaging for measurement of NAA in head injured patients.** *Acta Neurochir Suppl* 2002;81:373–375
23. Govindaraju V, Gauger GE, Manley GT, Ebel A, Meeker M, and Maudsley AA. **Volumetric proton spectroscopic imaging of mild traumatic brain injury.** *AJNR Am J Neuroradiol* 2004;25:730–737
24. Pouwels PJ, Brockman K, Kruse B, et al. **Regional age dependence of human brain metabolites from infancy to adulthood as detected by quantitative localized proton MRS.** *Pediatr Res* 1999;46:474–485
25. Kreis R, Ernst T, Ross BD. **Development of the human brain: *in vivo* quantification of metabolite and water content with proton magnetic resonance spectroscopy.** *Magn Res Med* 1993;30:424–437
26. Haseler LJ, Phil M, Arcinue E, Danielsen ER, Bluml S, Ross BD. **Evidence from proton magnetic resonance spectroscopy for a metabolic cascade of neuronal damage in shaken baby syndrome.** *Pediatrics* 1997;99:4–14
27. Fiser DH. **Assessing the outcome of pediatric intensive care.** *J Pediatr* 1992;121:68–74
28. Fiser DH, Long N, Roberson PK, Hefley G, Zolten K, Brodie-Fowler M. **Relationship of pediatric overall performance category and pediatric cerebral performance category scores at pediatric intensive care unit discharge with outcome measures collected at hospital discharge and 1- and 6-month follow-up assessments.** *Crit Care Med* 2000;28:2616–2620
29. Reichenbach JR, Venkatesan R, Schillinger DJ, Kido DK, Haacke EM. **Small vessels in the human brain: MR venography with deoxyhemoglobin as an intrinsic contrast agent.** *Radiology* 1997;204:272–277
30. Gennarelli TA, Thibault LE, Adams JH, Graham DI, Thompson CJ, Marcincin RP. **Diffuse axonal injury and traumatic coma in the primate.** *Ann Neurol* 1982;12:564–574
31. Garnett MR, Blamire AM, Corkill RG, Cadoux-Hudson TAD, Rajagopalan B, Styles P. **Early proton magnetic resonance spectroscopy in normal-appearing brain correlates with outcome in patients following traumatic brain injury.** *Brain* 2000;123:2046–2054
32. Shutter L, Tong KT, Colohan A, Holshouser BA. **Serial quantitative proton spectroscopic findings in severely brain injured patients correlate with outcomes.** Presented at: First Joint Symposium of the National and International Neurotrauma Societies, Tampa, FL, October 27–November 1, 2002
33. Brooks WM, Stidley CA, Petropoulos H, et al. **Metabolic and cognitive response to human traumatic brain injury: a quantitative proton magnetic resonance study.** *J Neurotrauma* 2000;17:629–640
34. Danielsen ER, Christensen PB, Arlien-Soborg P, Thomsen C. **Axonal recovery after severe traumatic brain injury demonstrated in vivo by 1H MR spectroscopy.** *Neuroradiology* 2003;45:722–724
35. Freidman SD, Brooks WM, Jung RE, et al. **Quantitative proton MRS predicts outcome after traumatic brain injury.** *Neurology* 1999;52:1384–1391
36. Wild JM, Macmillan CSA, Wardlow JM, et al. **1H spectroscopic imaging of acute head injury-evidence of diffuse axonal injury.** *MAGMA* 1999;8:109–115

37. Condon B, Oluoch-Olunya D, Hadley D, Teasdale G, Wagstaff A. **Early 1H magnetic resonance spectroscopy of acute head injury: four cases.** *J Neurotrauma* 1998;15:563–571
38. Robertson NJ, Lewis RH, Cowan FM, et al. **Early increases in brain myo-inositol measured by proton magnetic resonance spectroscopy in term infants with neonatal encephalopathy.** *Pediatr Res* 2001;50:692–700
39. Ashwal S, Holshouser BA, Tong KT. **Proton spectroscopy detected myoinositol in children with traumatic brain injury.** *Pediatr Res* 2004;56:1–9
40. Ebel A, and Maudsley AA. **Improved spectral quality for 3D MR spectroscopic imaging using a high spatial resolution acquisition strategy.** *Magn Reson Imaging* 2003;21:113–120
41. Li BS, Babb JS, Soher BJ, Maudsley AA, Gonen O. **Reproducibility of 3D proton spectroscopy in the human brain.** *Magn Reson Med* 2002;47:439–446